

Epithelial-mesenchymal transition and bi- and multi-nucleated trophoblast cell formation in ovine conceptuses during the peri-implantation period

Ayami YAMADA¹⁾, Kaito OHTSUKI¹⁾, Natsumi SHIGA¹⁾, Jonathan A. GREEN²⁾, Yuta MATSUNO¹⁾ and Kazuhiko IMAKAWA¹⁾

¹⁾Research Institute of Agriculture, Tokai University, Kumamoto 862-8652, Japan

²⁾Animal Science Research Center, University of Missouri-Columbia, Columbia, MO 65211, USA

Abstract. Epithelial-mesenchymal transition (EMT), which is common in cancer metastasis, is also observed during developmental processes such as embryo implantation into the maternal endometrium in humans and rodents. However, this process has not been well characterized in the non-invasive type of implantation that occurs in ruminants. To understand whether EMT occurs in ruminant ungulates, ovine conceptuses (embryo plus extraembryonic membranes) from days 15 (P15: pre-attachment), 17 (P17: during attachment), and 21 (P21: post-attachment, day 0 = day of estrus) were evaluated. RNA-seq analysis revealed that the expression of EMT-related transcripts increased on P21. Real-time PCR and western blotting analyses indicated that levels of transcripts and proteins indicative of mesenchyme-related molecules increased on P21, but a minor expression of epithelium-related molecules remained. Immunohistochemical analysis revealed that E-cadherin (CDH1) was localized in the elongated trophoctoderm on P15 and P17. On P21, CDH1 was localized to the trophoctoderm and on the conceptus cells undergoing differentiation. Vimentin (VIM) was localized in the uterine stroma on P15 and P17, and its expression was observed at the edge of elongating trophoblast on P21. Further, it was found that some bi-nucleated trophoblast cells were present on P17; however, numerous bi- and multi-nucleated trophoblast cells on the uterine epithelium or next to the uterine stroma were found on P21. A minor expression of pregnancy-associated glycoprotein (PAG) transcripts was found on P15 and P17, but a definitive expression of PAGs, transcripts, and proteins was found on P21. Although further investigation is required, these observations indicate that bi-nucleated trophoblast cell formation begins on the day conceptus implantation to the maternal endometrium is initiated, followed by EMT in trophoblast cells. These results suggest that these sequential events are required if pregnancy is to be established in ruminants.

Key words: Epithelial-mesenchymal transition (EMT), Implantation, Pregnancy-associated glycoprotein (PAG), Sheep, Trophoblast

(J. Reprod. Dev. 68: 110–117, 2022)

Epithelial-mesenchymal transition (EMT) is a well-known event in cancer metastasis, organ development, wound healing, and invasive modes of conceptus implantation [1]. EMT is a cellular process in which epithelial cells acquire a mesenchymal nature, characterized by a loss of apical-basal cell polarity, cytoskeleton remodeling, cell-cell adhesion weakening, and acquisition of cell motility [1]. We previously observed that bovine conceptuses (embryo plus extraembryonic membranes) exhibited features of EMT on day 22 (day 0 = day of estrus), 2–3 days after the initiation of conceptus attachment to the uterine epithelium. During this period, trophoctodermal cells expressed mesenchymal markers such as vimentin (VIM) and N-cadherin (CDH2), while expression of the epithelial cell marker cytokeratin was maintained. However, it is still not fully understood why non-invasive, ruminant trophoblasts undergo EMT at the time of conceptus adhesion to the uterine endometrium.

These observations were supported by results from *in vitro* cell

culture experiments in which bovine trophoblast CT-1 cells [3] were co-cultured with bovine endometrial epithelial cells [4, 5]. Endometrial follistatin was shown to decrease the effect of the potent EMT inducer activin A. These results were further supported by the observation that activin A expression increased when follistatin expression was downregulated on day 22 [4]. Furthermore, the expression of an EMT-related transcription factor, ovo-like zinc finger 2 (OVOL2), was elevated on day 20. As OVOL2 expression declined on day 22, the expression of other EMT-related transcription factors such as zinc finger E-box binding homeobox 1 (ZEB1) and snail family transcriptional repressor 1 (SNAI2) increased, as did VIM, a phenotypic marker for mesenchymal cells [5]. Collectively, these observations suggest that EMT occurs in bovine species during conceptus adhesion to the uterine endometrium.

It has been well documented that bi- and multi-nucleated trophoctodermal cells begin to form during the peri-implantation period in ruminants [6]. These cells are responsible for establishing syncytial plaques at the placenta-uterine interface. They can also express large amounts of secreted proteins, such as placental lactogen, prolactin-related proteins, and pregnancy-associated glycoproteins (PAGs) [7, 8]. Placental PAG expression is restricted to species within the order Cetartiodactyla (even-toed ungulates) [8]. Most PAG genes are present in the family Bovidae [9]. Cattle and sheep have more than two dozen intact PAG genes each, most of which are expressed locally

Received: July 16, 2021

Accepted: December 7, 2021

Advanced Epub: January 3, 2022

©2022 by the Society for Reproduction and Development

Correspondence: K Imakawa (e-mail: ik459102@tsc.u-tokai.ac.jp)

This is an open-access article distributed under the terms of the Creative Commons Attribution Non-Commercial No Derivatives (by-nc-nd) License. (CC-BY-NC-ND 4.0: <https://creativecommons.org/licenses/by-nc-nd/4.0/>)

in bi- and multi-nucleated trophoblasts [8]. Consequently, PAGs can serve as useful markers of ruminant trophoblasts, especially in the identification of bi- and multi-nucleated cells in the placenta [10].

Based on these observations, we hypothesized that EMT and trophoblast cell fusion are integral parts of the conceptus implantation processes required for subsequent placental formation in ruminants. In this study, we examined whether EMT-related transcripts and proteins were expressed *in utero* on days 15 (P15: pre-attachment), 17 (P17: during attachment), and 21 (P21: post-attachment) of gestation (day 0 = day of estrus) in the ovine species. We then determined the presence of bi- and multi-nucleated cells and the expression of PAGs in the maternal-fetal compartments.

Materials and Methods

Collection of ovine conceptuses/endometrial tissues and whole uterus fixation

The protocol for sheep experimentation with whiteface crossbred ewes, maintained at the farm of the University of Tennessee, Knoxville, TN, USA, was reviewed and approved by the Animal Care Committee of the University of Tennessee, the University of Tokyo, and Tokai University (approval number: 20-017-23). Animal husbandry, estrous synchronization, and tissue collection were performed as described previously [11]. For uterine fixation, hysterectomy was performed on P15, P17, and P21, and the uteri (n = 3 each) were subjected to whole uterus fixation within 15 min after slaughter [12]. Fixed whole uteri that were paraffin-embedded, and frozen conceptuses and endometria were initially transferred to the Laboratory of Animal Breeding, The University of Tokyo, and then transferred to Tokai University, Kumamoto, Japan. The fixed and paraffin-embedded uterine tissue blocks were sectioned (6 µm), stained with hematoxylin and eosin, and evaluated for intra-uterine structures, including the presence of conceptuses [13].

RNA-sequencing analysis

The original RNA-seq datasets from P15, P17, and P21 ovine conceptuses (n = 4/day each) have been previously reported [14] and deposited in the Data Bank of Japan (DDBJ, DRA011433 and DRA011655, <http://www.ddbj.nig.ac.jp>). The sequences were pseudoaligned, and transcripts were quantified using RaNA-seq (a bioinformatics tool for the analysis of RNA-seq data, <https://ranaseq.eu/index.php>) with its default parameters [15]. The transcripts encoding the EMT GO term (GO: 0001837) were then extracted and subjected to heatmap analysis using iDEP [16]. Transcripts encoding PAGs (*PAG1*, ensemble ID: ENSOARG00000008858, *PAG3*, ensemble ID: ENSOARG00000004722, *PAG4*, ensemble ID:

ENSOARG00000006110, *PAG5*, ensemble ID: ENSOARG00000000700, *PAG6*, ensemble ID: ENSOARG00000011295, *PAG7*, ensemble ID: ENSOARG00000008931, and *PAG10*, ensemble ID: ENSOARG00000008256) were extracted and the expression values are shown in the normalized form of transcripts per million (TPM) [17].

Quantitative reverse-transcription (RT)-PCR analysis

Using ISOGEN II (311-07361; NIPPON GENE Co., Ltd., Tokyo, Japan), total RNA was extracted from P15, P17, and P21 frozen sheep conceptuses (n = 3/day) according to the manufacturer's protocol. For real-time PCR, isolated RNA (1 µg) was reverse-transcribed to cDNA using a ReverTra Ace qPCR RT Master Mix (FSQ-301; Toyobo, Osaka, Japan) according to the manufacturer's instructions. Three microliters of each prepared cDNA, diluted 1:10 in DNase- and RNase-free water, was subjected to real-time PCR amplification using a Thunderbird SYBR qPCR Mix Kit (QPS-201; Toyobo) on a StepOnePlus real-time PCR system (Thermo Fisher Scientific K.K., Tokyo, Japan). The primers used are listed in Table 1. The amplification efficiencies of each target and the reference gene, ovine beta-actin (*ACTB*), were examined through their calibration curves and were found to be comparable [4,5]. The thermal profile consisted of 40 cycles at 95°C for 15 sec and annealing and extension at 60°C for 60 sec. The average threshold (Ct) values for each target were determined as described previously [4]. Melting curve analysis was performed for each run to confirm the specificity of amplification and the absence of primer dimers [4]. The expression levels of the transcripts were normalized to the levels of the reference gene, *ACTB*, using the $2^{-\Delta\Delta Ct}$ method [18].

Protein extraction and western blotting

Western blot analysis was performed using frozen P15, P17, and P21 sheep conceptuses (n = 3 each). Tissue lysates (15 µg) were mixed with a sample buffer solution (2ME+, 2 ×) [4% SDS, 10% 2-mercaptoethanol, 20% glycerol, 0.002% bromophenol blue, and 0.125 M Tris-HCl (196-11022; FUJIFILM Wako Pure Chemical Corporation Inc., Osaka, Japan)], and boiled for 4 min. Samples were loaded onto each lane, separated by 10% SDS-PAGE (acrylamide gel, 192-14961; FUJIFILM Wako Pure Chemical Corporation Inc.), and then transferred onto polyvinylidene difluoride membranes (IPVH00010; Merck KGaA, Darmstadt, Germany). The membranes were then blocked with Block ACE (UKB80; KAC Co., Kyoto, Japan) and treated with one of the following antibodies: rabbit anti-bovine cytokeratin antibody (1:1000, Z0622; Dako, Glostrup, Denmark), rabbit anti-human VIM antibody (1:1000, ab45939; Abcam, Tokyo, Japan), rabbit anti-human E-cadherin (CDH1) antibody (1:1000, #3195; Cell Signaling Technology, Danvers, MA, USA), rabbit

Table 1. Nucleotide sequences for primers used in this study

| Gene | Accession No. | Nucleotide sequence (5'-3') | | Length (bp) |
|--------------|----------------|-----------------------------|------------------------|-------------|
| | | Forward | Reverse | |
| <i>ACTB</i> | NM_001009784.3 | TCCTGGAGAAGAGCTACGA | GGGCAGTGATCTCTTCTGC | 256 |
| <i>KRT8</i> | XM_012174208.4 | AAACTCTGGCCAGGATAAGC | CTCCAGCTCTACCTTGTCATG | 179 |
| <i>CDH1</i> | XM_027978118.2 | CGCTCTCCAGGAACCTCTG | TTTGTGTGTGGCAGCATGG | 124 |
| <i>OVOL2</i> | XM_015099647.3 | AGGGCTTCAACGACACCTTC | TCGCAGACGTACAGCTTATCC | 190 |
| <i>VIM</i> | XM_004014247.5 | CAAGTCCAAGTTTGCTGACC | TCATGTTCTGAATCTCATCCTG | 245 |
| <i>CDH2</i> | XM_027960884.2 | ATGAGAGGCCCATCCATGC | AAGACTAAGAGGGAGTCGTAGG | 145 |
| <i>SNAI2</i> | NM_001126342.1 | CAAGGACACATCAGAACTCAC | CTCTTGCACTGGTATTCTTGAC | 134 |
| <i>ZEB1</i> | XM_027976675.2 | ATATTGCTATACCTACCGTCAC | TTGCCTTTCATCCTGATTCC | 212 |

anti-human CDH2 antibody (1:1000, ab18203; Abcam), or rabbit anti-human beta-actin antibody (1:5000, GTX109639; GeneTex, Irvine, CA, USA). The membranes were then incubated with a secondary antibody conjugated with horseradish peroxidase (goat anti-rabbit IgG antibody, 1:5000, PI-1000; Vector Laboratories Inc., Burlingame, CA, USA) diluted with Block ACE. Finally, proteins were detected using ImmunoStar LD (290-69904; FUJIFILM Wako Pure Chemical Corporation Inc.). Images were captured using a LuminoGraph2 system (WSE-6200H; ATTO Corporation Inc., Tokyo, Japan).

Immunohistochemical detection of epithelial and mesenchymal markers, bi-/multi-nucleate cells, followed by immunofluorescence analysis

Immunohistochemical analysis was performed on paraffin sections (6 μ m) of the P15, P17, and P21 uterine tissue. Paraffin sections were rehydrated, boiled for 15 min in 10 mM citrate buffer (pH 6.0), and then blocked in 10% normal goat serum (S-1000; Vector Laboratories, Inc.) for 1 h at room temperature. The sections were incubated overnight at 4°C with the following primary antibodies: rabbit anti-human VIM antibody (1:400, ab45939; Abcam), rabbit anti-human CDH1 antibody (1:400, #3195; Cell Signaling Technology), and rabbit anti-bovine PAG antibody (20 μ g/ml, polyclonal). This PAG antibody was raised against a purified PAG preparation that consisted primarily of bovine PAG4 and PAG6 (modern-grouped PAGs) [19]. Antibody dilution was optimized prior to this study. The same concentration of normal rabbit IgG (553-61281; R&D Systems, Tokyo, Japan) was used as a negative control. Immunoreactive proteins were detected using a FITC-conjugated goat anti-rabbit IgG (H+L) antibody (SA00003-2; Proteintech Group Inc., Rosemont, IL, USA) at a dilution of 1:100 for 1 h at room temperature. Tissues were then washed twice for 5 min per wash in PBST [pH 7.4, 0.14 M sodium chloride, 0.0027 M potassium chloride, 0.01 M phosphate (5000125; TOHO K.K., Tokyo, Japan), 0.1% Tween-20 (23926-35; Nacalai TESQUE Inc., Kyoto, Japan)] and once for 5 min in PBS (5000125; TOHO K.K.). Slides were counterstained with VECTASHIELD Hard/ Set Mounting Medium with DAPI (H-1500; Vector Laboratories Inc.), and coverslips were overlaid. Images were taken using an ALL-IN-ONE immunofluorescence microscope (BZ-X800; Keyence, Osaka, Japan).

Statistical analysis

All experiments were repeated independently at least three times. Statistical analyses were conducted using RStudio (Version 3.5.3), and the significance of each pairwise comparison was assessed using the Tukey-Kramer test. Statistical significance was set at $P < 0.05$.

Results

Expression of EMT-related transcripts in conceptuses during the peri-implantation period

From our previous RNA-sequencing data [14], EMT-related transcripts were extracted, their expression was evaluated, and heatmap analysis was performed. The heatmap analysis revealed that transcripts encoding EMT-related genes were distinctively upregulated in P21 ovine conceptuses (Fig. 1). These analyses indicated that the increase in EMT-related transcripts and conceptus adhesion appeared to occur simultaneously in ovine conceptuses on P21 [14].

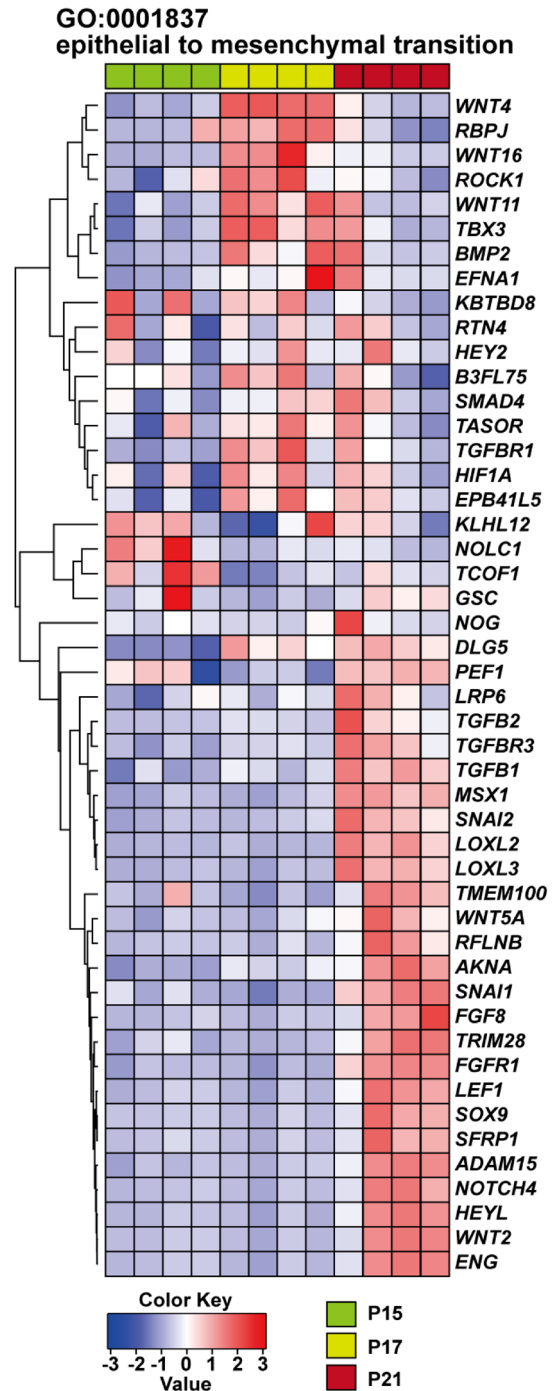


Fig. 1. Expression of transcripts encoding the EMT GO term (GO:0001837) in ovine conceptuses. A heatmap analysis of the EMT-related transcripts in P15, P17, and P21 conceptuses ($n = 4$ each day) is shown. Upregulated transcripts are shown in red, and downregulated transcripts are shown in blue. While some EMT-related molecules are upregulated on P17, many of those are upregulated in P21 conceptuses.

RT-qPCR, western blot, and immunohistochemical analyses of EMT-related factors in ovine conceptuses

Next, we examined the expression of EMT-related transcripts and proteins in P15, P17, and P21 ovine conceptuses. Quantitative PCR demonstrated the downregulation of cytokeratin (as *KRT8*), *CDH1*, and *OVOL2* on P21, while there was an upregulation of *VIM*, *CDH2*,

SNAI2, and *ZEB1* (Fig. 2A). These results are in agreement with previous reports [2, 4, 5].

Western blotting analysis revealed that cytokeratin and CDH1 levels decreased but were still present on P21, while CDH2 and VIM expression was only seen on P21 (Fig. 2B). The expression of CDH1 and VIM on these days was also confirmed through immunohistochemical analyses (Fig. 3). Although CDH1 expression was confined to the trophoblast on P15 and P17, its expression on P21 appeared at the apical side of the trophoblast, opposite to the attachment side. On P15 and P17, VIM expression was found in the stromal region, excluding the glandular epithelium or blood vessels. On P21, however, VIM expression appeared at the apical side of the trophoblast as well as at the edge of the trophoblast undergoing possible cellular differentiation.

Determining the presence of bi- or multi-nucleated trophoblasts and expression of PAG transcripts, followed by immunohistochemical and immunofluorescence detection of PAG expression in ovine conceptuses

Immunohistochemical analysis revealed that some bi-nucleated trophoblast cells were detected on P17, but definitive bi- and multi-nucleated trophoblast cells, located on the uterine epithelial cells or next to the uterine stroma, were found on P21 (Figs. 3 and 5A).

From our previous RNA-sequencing data [14], *PAG* transcripts were extracted, and their expression patterns were analyzed (Fig. 4). Minute expression of *PAG* transcripts was found on P15 and P17,

but an increase in *PAG* transcripts was observed on P21.

Immunohistochemical detection also revealed that while *PAG* expression was rarely found on P15, there were two patterns of *PAG* expression, presence or absence, in P17 conceptuses. Similar to *PAG* transcripts, distinct *PAG* expression was observed on P21 (Fig. 5A). These findings were confirmed via immunofluorescence analysis, in which *PAG* expression was associated with bi- and multi-nucleated trophoblast cells (Figs. 5B and 5C). It should be noted that bi- or multi-nucleated cells were not detected in the endometrial-stromal compartments on P15, P17, or P21 (Fig. 3 and Fig. 5).

Discussion

We demonstrated that, similar to bovine conceptuses [2, 4, 5], sheep conceptuses underwent epithelial-mesenchymal transition (EMT) on P21, 3–4 days after the initial attachment of the trophoblast to the uterine epithelium. Although sheep conceptuses expressed morphological and functional mesenchymal markers, VIM and CDH2, respectively, on P21, they also expressed epithelial markers such as cytokeratin and CDH1 on the same day. In particular, VIM expression in P21 conceptuses was restricted to the apical side, opposite the conceptus attachment to the uterine epithelium or the edge of the developing trophoblast. In contrast, CDH1 expression was found in conceptuses undergoing differentiation; thus, the trophoblast cells that express VIM or CDH1 appear to differ. Yang *et al.* [1] provided a consensus statement in their EMT plasticity model that

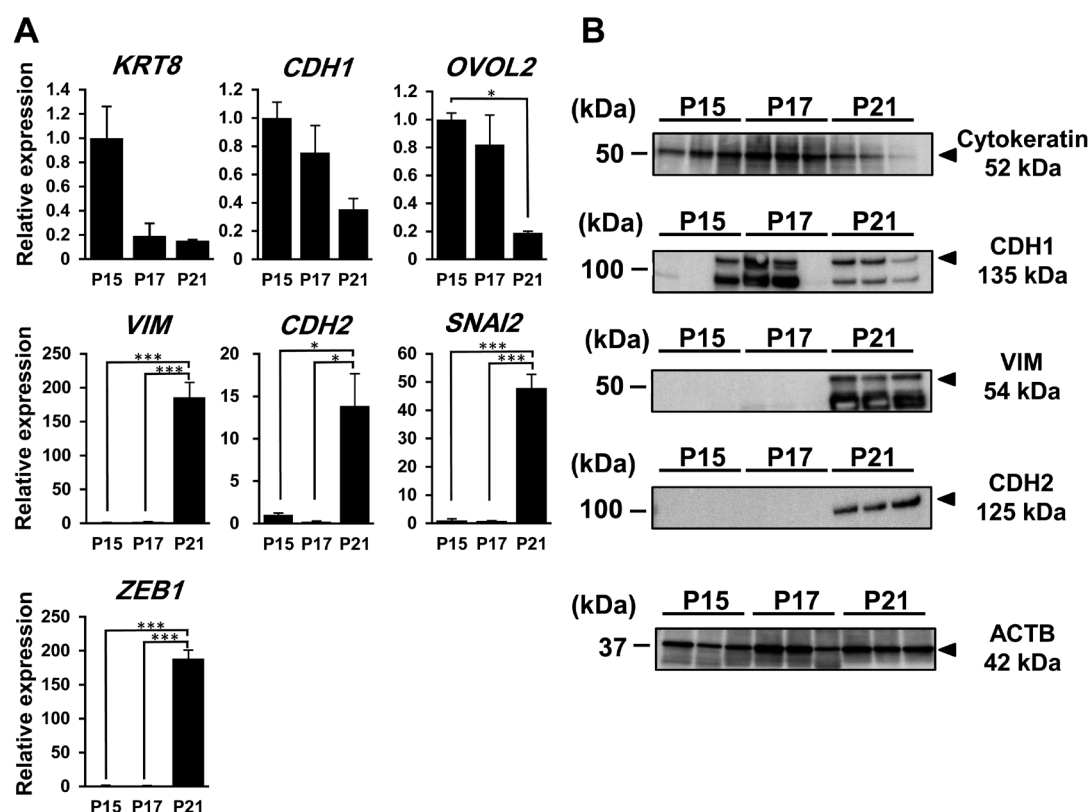


Fig. 2. Expression of EMT-related transcripts and proteins in ovine conceptuses during the peri-implantation period. (A) RT-qPCR analysis of transcripts encoding EMT-related factors in P15, P17, and P21 ovine conceptuses. RNA was extracted from frozen conceptuses ($n = 3/\text{day}$). Data relative to the value of P15 are shown. Values represent the means \pm SEM. *ACTB* was used as the reference gene. *** $P < 0.001$, * $P < 0.05$. (B) Western blot analysis of EMT-related proteins in P15, P17, and P21 ovine conceptuses ($n = 3/\text{day}$). While VIM and CDH2 are expressed only on P21, some epithelial markers, such as cytokeratin and CDH1, are expressed on P21. The numbers on the left denote the molecular weight markers, while those on the right are the product sizes. ACTB was used as the loading control.

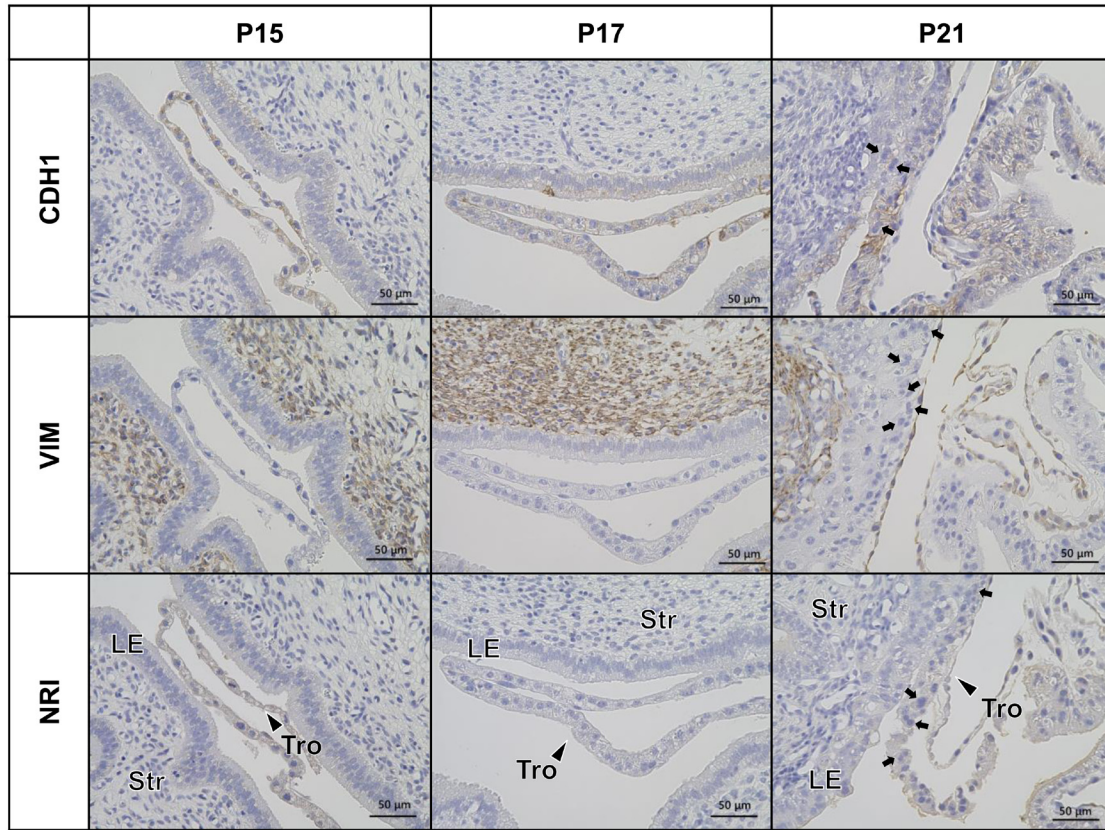


Fig. 3. Expression of the epithelial marker CDH1 and the mesenchymal marker VIM in P15, P17, and P21 ovine uteri. Tissue sections of P15, P17, or P21 ovine uteri were stained with anti-CDH1 or anti-VIM antibodies. Top: Cellular CDH1 localization in P15, P17, and P21 uteri. Middle: VIM localization in P15, P17, and P21 uteri. Bottom: NRI, Normal Rabbit IgG (negative control). CDH1 was localized in the elongated trophoctoderm on P15 and P17. On P21, CDH1 was localized on the trophoctoderm and the conceptus cells undergoing differentiation. VIM was localized in the uterine stroma on P15, P17, and P21. In addition, VIM expression was seen at the edge of the developing conceptuses on P21. LE: luminal epithelium of the endometrium, Str: uterine stroma, Tro: trophoblast. Arrowheads indicate the trophoblast and the small arrows indicate bi-nucleated cells. Scale bar = 50 μ m.

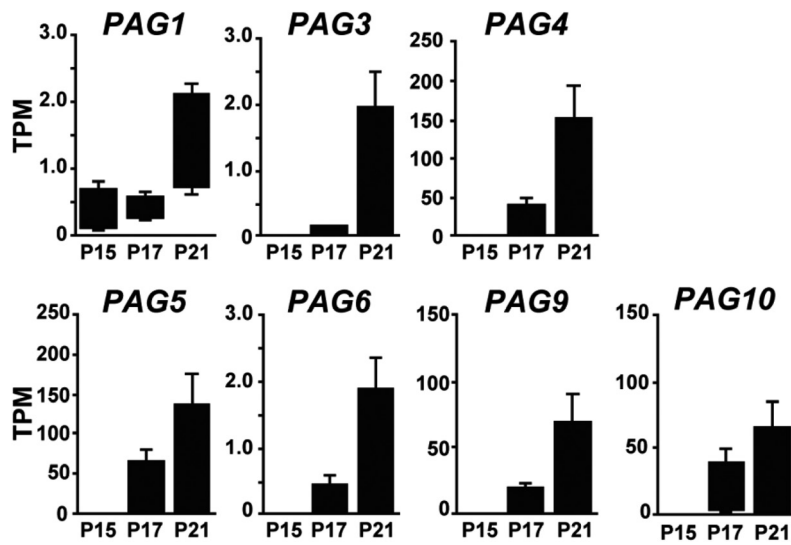


Fig. 4. Expression of pregnancy-associated glycoprotein (PAG)-related transcripts in ovine conceptuses. From the RNA-seq analysis done previously [14], PAG-related transcripts were extracted and their expression values were shown as transcripts per million (TPM). Transcripts encoding various PAG genes, *PAG1*, *PAG3*, *PAG4*, *PAG5*, *PAG6*, *PAG9*, and *PAG10*, were found, particularly on P21. TPM: transcripts per million.

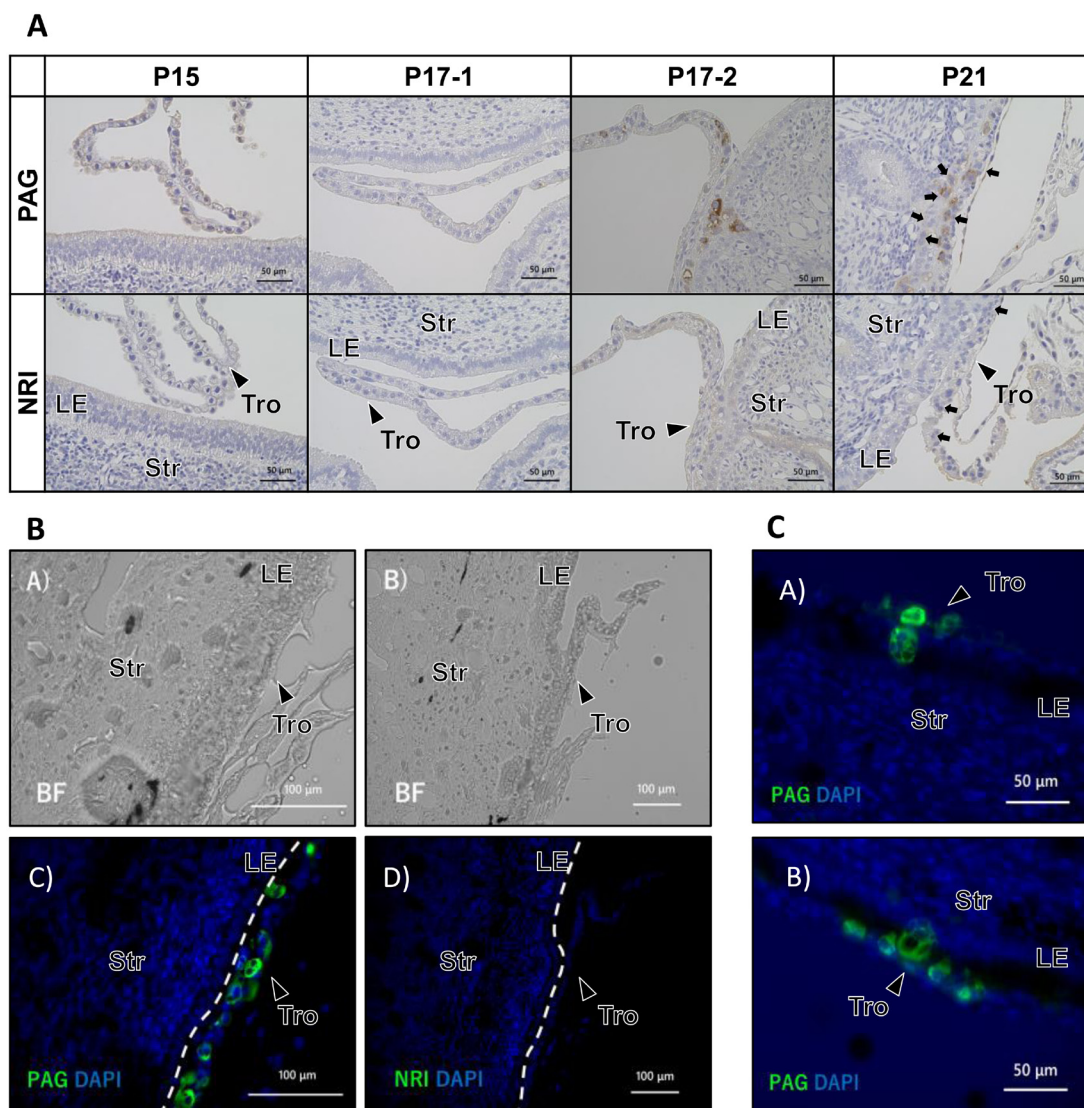


Fig. 5. Presence of bi- and multi-nucleated cells at the maternal-fetal compartments and the expression of pregnancy-associated glycoproteins (PAGs). The rabbit antibody used in this study was raised against purified bovine PAG4 and PAG6, which detects bi- and multi-nucleated ovine trophoblast cells [18]. A: Immunohistochemical analysis and localization of PAG in P15, P17, and P21 uteri. As seen in Fig. 3, a few bi-nucleated trophoblast cells are present in P17 uteri, and distinctive bi- and multi-nucleated trophoblast cells exist in P21 uteri. There are two patterns of PAG expression on P17, one with PAG expression and the other without PAG expression; however, definitive PAG expression was seen on P21. Arrowheads indicate trophoblasts and small arrows indicate bi-nucleated cells. B: Immunofluorescence study of PAG expression in the P21 ovine uterus. A) and B) are bright-field images (BF) of PAG expression in C) and the control with normal rabbit IgG in D), respectively. The dotted white line indicates the separation between the trophoblast layer from the maternal tissues. Note that trophoblast cells are located next to the uterine epithelial layer in C). C: Various bi- and multi-nucleated trophoblasts are found in P21 uteri, all of which are associated with PAG expression. These cells were found next to the stroma as if they invaded the epithelial cells and replaced them, but trophoblast cells were not found within the stroma. LE: luminal epithelium of the endometrium, Str: uterine stroma, Tro: trophoblast. Scale bars = 50 μ m or 100 μ m.

there are cells with epithelial/mesenchymal (E/M) intermediate states in addition to the distinct epithelial and mesenchymal cells. In this study, some bi-nucleated cells appeared in P17 trophoblasts; however, distinctive bi- and multi-nucleated cells were found on P21. Although the molecular and cellular mechanisms in which EMT is required for multi-nucleated cell fusion or for when the two events occur simultaneously in P21 trophoblasts have not yet been elucidated, the observations in which P21 sheep trophoblasts undergo intermediate EMT suggest that they could have reduced cell-cell adhesion, increased cell individualization, or the acquisition of cell motility, possibly allowing active cell fusions between neighboring trophoblast cells.

The cellular mechanisms associated with the formation of bi- and multi-nucleated trophoblast cells from mononucleated cells are not well understood; however, two theories on trophoblast cell fusions currently exist: consecutive nuclear divisions without cytokinesis (mitotic polyploidy) [20] or the fusion of mononucleated trophoblast cells [21]. Among the numerous bi- and multi-nucleated trophoblast cells detected in our tissue sample sets, we did not find any fused cells containing both conceptus and endometrial origins or those in the endometrial-stromal compartments. This does not agree with those found in bovine species, wherein tri- or multi-nucleated cells of the trophoblast and uterine epithelial origins often appear in the uterine endometrium [22]. However, our results agree with those

from a recent publication [23], wherein fused cells comprised all trophoctodermal cells in sheep. Although a definitive conclusion on the cell fusion between trophoctodermal and maternal cells could not be made, the results from two studies ([23] and this study) could challenge those believed for the last 40 years in which tri- or multi-nucleated cells result from the fusion between one endometrial epithelial and one bi-nucleate trophoctodermal cell.

We found that *PAG* transcripts were minutely expressed in P15 conceptuses and their expression slightly increased on P17. However, major *PAG* expression was found when bi- and multi-nucleated trophoblast cells were present on P21. Our previous proteome studies demonstrated that a predicted PAG2-like protein was detected in P15 ovine uterine flushing media, the expression of which increased on P17 [14]. In addition, the PAG proteins, PAG4 and PAG8, were detected in the uterine flushing media from P17 and P20 bovine uteri [4]. It should be noted that PAG expression is routinely found in the maternal circulation; thus, PAG expression is likely confined in the uterus until the conceptus adheres to the maternal endometrium. Based on our previous [4] and present experiments, PAG expression appeared prior to EMT; however, the elucidation of the functional relationship between these two events is beyond the scope of the current investigation.

In this study, bi- and multi-nucleated cells with PAG expression were often located in the epithelial layer next to the uterine stroma, as if multi-nucleated trophoctodermal cells had replaced the uterine epithelial cells. To determine whether the disappearance of uterine epithelial cells was due to cell apoptosis, we attempted to identify the *in utero* expression of the apoptosis inducer caspase 3, followed by detecting DNA degradation through the TUNEL assay. Although minute expression of caspase 3 in one of the four sheep uteri examined was found in the epithelial cells, we did not find any TUNEL-positive staining (unpublished observations). Unlike the TUNEL-positive cells found previously by others [23], who concluded that the trophoblast could have triggered apoptosis in uterine epithelial cells, our data do not support this notion. Furthermore, the disappearance of uterine epithelial cells was observed during the implantation processes in mice; however, the mechanisms of epithelial cell removal, apoptosis, or necrosis have not been established [24]. Results from previous and present studies suggest that further investigation is required to determine the molecular and cellular mechanisms associated with conceptus implantation processes such as uterine epithelial cell removal, trophoblast EMT, and cell fusion beyond conceptus attachment and adhesion to the uterine endometrium.

Conclusion

We found that sheep conceptuses undergo epithelial-mesenchymal transition (EMT) during the period in which conceptus adhesion to the uterine epithelium takes place several days after the initiation of conceptus implantation to the maternal endometrium. Bi-nucleated cell formation and PAG expression begin before EMT, but the increase in the frequency of these events was found on day 21, coincident with EMT events in the trophoctoderm in ruminants.

Conflict of interests: The authors declare that there are no conflicts of interest that could be perceived as prejudicing the impartiality of the research reported.

Acknowledgments

This work was supported by a Grant-in-Aid for Scientific Research (16H02584) from the Japan Society for the Promotion

of Science (JSPS) and by the Livestock Promotional Funds of the Japan Racing Association (JRA). Support for immunohistochemical analysis was provided by the staff at the Support Center for Medical Research and Education, Tokai University. The authors are grateful to Dr. James D. Godkin (retired from the University of Tennessee) for collecting the sheep samples used in this study. The authors also thank Dr. Kazuya Kusama of the Tokyo University of Pharmacy and Life Sciences and Ms. Tomoka Iwata of Tokai University for the laboratory method training and preparation of the manuscript, respectively.

References

- Yang J, Antin P, Berx G, Blanpain C, Brabletz T, Bronner M, Campbell K, Cano A, Casanova J, Christofori G, Dedhar S, Derynck R, Ford HL, Fuxe J, Garcia de Herreros A, Goodall GJ, Hadjantonakis AK, Huang RYJ, Kalchauer C, Kalluri R, Kang Y, Khew-Goodall Y, Levine H, Liu J, Longmore GD, Mani SA, Massagué J, Mayor R, McClay D, Mostov KE, Newgreen DF, Nieto MA, Puisieux A, Runyan R, Savagner P, Stanger B, Stemmler MP, Takahashi Y, Takeichi M, Theveneau E, Thiery JP, Thompson EW, Weinberg RA, Williams ED, Xing J, Zhou BP, Sheng G. EMT International Association (TEMTIA). Guidelines and definitions for research on epithelial-mesenchymal transition. *Nat Rev Mol Cell Biol* 2020; 21: 341–352. [Medline] [CrossRef]
- Yamakoshi S, Bai R, Chaen T, Ideta A, Aoyagi Y, Sakurai T, Konno T, Imakawa K. Expression of mesenchymal-related genes by the bovine trophoctoderm following conceptus attachment to the endometrial epithelium. *Reproduction* 2012; 143: 377–387. [Medline] [CrossRef]
- Talbot NC, Caperna TJ, Edwards JL, Garrett W, Wells KD, Ealy AD. Bovine blastocyst-derived trophoctoderm and endoderm cell cultures: interferon tau and transferrin expression as respective *in vitro* markers. *Biol Reprod* 2000; 62: 235–247. [Medline] [CrossRef]
- Kusama K, Bai R, Ideta A, Aoyagi Y, Okuda K, Imakawa K. Regulation of epithelial to mesenchymal transition in bovine conceptuses through the interaction between follistatin and activin A. *Mol Cell Endocrinol* 2016; 434: 81–92. [Medline] [CrossRef]
- Bai R, Kusama K, Nakamura K, Sakurai T, Kimura K, Ideta A, Aoyagi Y, Imakawa K. Down-regulation of transcription factor OVOL2 contributes to epithelial-mesenchymal transition in a noninvasive type of trophoblast implantation to the maternal endometrium. *FASEB J* 2018; 32: 3371–3384. [Medline] [CrossRef]
- Imakawa K, Bai R, Kusama K. Integration of molecules to construct the processes of conceptus implantation to the maternal endometrium. *J Anim Sci* 2018; 96: 3009–3021. [Medline] [CrossRef]
- Patel OV, Yamada O, Kizaki K, Todoroki J, Takahashi T, Imai K, Schuler LA, Hashizume K. Temporospatial expression of placental lactogen and prolactin-related protein-1 genes in the bovine placenta and uterus during pregnancy. *Mol Reprod Dev* 2004; 69: 146–152. [Medline] [CrossRef]
- Wallace RM, Pohler KG, Smith MF, Green JA. Placental PAGs: gene origins, expression patterns, and use as markers of pregnancy. *Reproduction* 2015; 149: R115–R126. [Medline] [CrossRef]
- Telugu BP, Walker AM, Green JA. Characterization of the bovine pregnancy-associated glycoprotein gene family—analysis of gene sequences, regulatory regions within the promoter and expression of selected genes. *BMC Genomics* 2009; 10: 185. [Medline] [CrossRef]
- Wooding FB. The role of the binucleate cell in ruminant placental structure. *J Reprod Fertil Suppl* 1982; 31: 31–39. [Medline]
- Sakurai T, Bai H, Konno T, Ideta A, Aoyagi Y, Godkin JD, Imakawa K. Function of a transcription factor CDX2 beyond its trophoctoderm lineage specification. *Endocrinology* 2010; 151: 5873–5881. [Medline] [CrossRef]
- Imakawa K, Ji Y, Yamaguchi H, Tamura K, Weber LW, Sakai S, Christenson RK. Co-expression of transforming growth factor β and interferon τ during peri-implantation period in the ewe. *Endocr J* 1998; 45: 441–450. [Medline] [CrossRef]
- Imakawa K, Imai M, Sakai A, Suzuki M, Nagaoka K, Sakai S, Lee S-R, Chang K-T, Echterkamp SE, Christenson RK. Regulation of conceptus adhesion by endometrial CXC chemokines during the implantation period in sheep. *Mol Reprod Dev* 2006; 73: 850–858. [Medline] [CrossRef]
- Matsuno Y, Amin YA, Kusama K, Imakawa K. Formation of fibrin at sights of conceptus adhesion in the ewe. *Reproduction* 2021; 161: 709–720. [Medline] [CrossRef]
- Prieto C, Barrios D. RaNA-Seq: Interactive RNA-Seq analysis from FASTQ files to functional analysis. *Bioinformatics* 2019; 36: 1955–1956. [Medline]
- Ge SX, Son EW, Yao R. iDEP: an integrated web application for differential expression and pathway analysis of RNA-Seq data. *BMC Bioinformatics* 2018; 19: 534. [Medline] [CrossRef]
- Wagner GP, Kin K, Lynch VJ. Measurement of mRNA abundance using RNA-seq data: RPKM measure is inconsistent among samples. *Theory Biosci* 2012; 131: 281–285. [Medline] [CrossRef]

18. **Livak KJ, Schmittgen TD.** Analysis of relative gene expression data using real-time quantitative PCR and the 2(-Delta Delta C(T)) Method. *Methods* 2001; **25**: 402–408. [[Medline](#)] [[CrossRef](#)]
19. **Green JA, Xie S, Quan X, Bao B, Gan X, Mathialagan N, Beckers J-F, Roberts RM.** Pregnancy-associated bovine and ovine glycoproteins exhibit spatially and temporally distinct expression patterns during pregnancy. *Biol Reprod* 2000; **62**: 1624–1631. [[Medline](#)] [[CrossRef](#)]
20. **Klisch K, Hecht W, Pfarrer C, Schuler G, Hoffmann B, Leiser R.** DNA content and ploidy level of bovine placentomal trophoblast giant cells. *Placenta* 1999; **20**: 451–458. [[Medline](#)] [[CrossRef](#)]
21. **Dunlap KA, Palmarini M, Spencer TE.** Ovine endogenous betaretroviruses (enJSRVs) and placental morphogenesis. *Placenta* 2006; **27**(Suppl A): S135–S140. [[Medline](#)] [[CrossRef](#)]
22. **Wooding FB, Burton G.** Synepitheliochorial placentation: Ruminants (ewe and cow). In: Wooding, F.B.P., Burton, G., (eds.), *Comparative Placentation: Structures, Functions and Evolution*. Berlin, Germany: Springer; 2008: 133–167.
23. **Seo H, Bazer FW, Burghardt RC, Johnson GA.** Immunohistochemical examination of trophoblast syncytialization during early placentation in sheep. *Int J Mol Sci* 2019; **20**: 4530. [[Medline](#)] [[CrossRef](#)]
24. **Akaeda S, Hirota Y, Fukui Y, Aikawa S, Shimizu-Hirota R, Kaku T, Gebril M, Hirata T, Hiraoka T, Matsuo M, Haraguchi H, Saito-Kanatani M, Takeda N, Fujii T, Osuga Y.** Retinoblastoma protein promotes uterine epithelial cell cycle arrest and necroptosis for embryo invasion. *EMBO Rep* 2021; **22**: e50927. [[Medline](#)] [[CrossRef](#)]